International Journal of Shape Modeling

ON 2D SOLID α-COMPLEXES OF POISSON DISC SAMPLINGS

ESDRAS MEDEIROS, LUIZ VELHO

IMPA–Instituto de Matemática Pura e Apicada,
Visgraf Laboratory, Estrada D. Castorina 110
Rio de Janeiro, RJ, 22460-320, Brazil
{*esdras, lvelho*}*@visgraf.impa.br*

HÉLIO LOPES AND THOMAS LEWINER

PUC-RIO–Pontifícia Universidade Católica do Rio de Janeiro,
MatMídia Laboratory, Rua Marques de São Vicente
Rio de Janeiro, RJ, 22.453-900, Brazil
{*lopes, tomlew*}*@mat.puc-rio.br*

Received (Day Month Year)
Revised (Day Month Year)
Accepted (Day Month Year)

Communicated by (xxxxxxxxxx)

This paper studies triangulations obtained from Poisson disc sampling. The Poisson disc sampling strategy with radius parameter α can be used to obtain a set of points in the interior or on the boundary of a given solid object in the plane. Using this sampling, one can construct a triangulation from its α-complex. In this work we give two contributions: the quality of this triangulation in terms of triangles' aspect ratio and a sampling condition with topological guarantee. If we choose the same parameter α for the Poisson disc sampling and for the solid α-complex, we prove that all the triangles in the complex have aspect ratio less or equal than $4\sqrt{3}$, which is only three times the aspect ratio of an equilateral triangle. Moreover, we prove that this bound is tight. We also establish a condition on radius parameter α that allows to recover, with topological guarantees, the original solid object from the α-complex representation.

Keywords: Poisson Disc Sampling; Mesh Quality; Sampling Condition.

1. Introduction

Fundamental problems in computer graphics and scientific simulation involve sampling issues. The properties of the sampling distributions greatly affect the quality of the final result, either in terms of simulation accuracy or visual aesthetic. Among geometrical samplings, the Poisson disc sampling strategy generates uniformly distributed points, ensuring a maximal and minimal distance between two close samples. It mimics the distribution of photo receptors in a primate eye[3], and is an excellent example of blue noise[2]. Such properties have made it widely used in Computer Graphics[16].

Mesh generation from points (particularly triangulations), is an important step in scientific and engineering applications. It is well known that the accuracy of finite element methods (FEM) is strongly dependent on the quality of the mesh elements[21]. A popular quality measure that we will study in this paper is the aspect-ratio of triangles[9,11].

Problem description Consider a solid object $\mathcal{O}$ in the plane. Using a Poisson disc sampling strategy, with radius parameter α, one can obtain a set of points $\mathcal{P}_\alpha$ that lies in the interior or on the boundary of $\mathcal{O}$. From $\mathcal{P}_\alpha$, one can construct a solid α-complex $\mathcal{C}_\alpha$. This kind of mesh is obtained by removing from the Delaunay triangulation, all triangles that have circumradius greater than a fixed positive real parameter α.

Contributions Let us take the measure of the aspect ratio of the triangle τ as $(\frac{L^2}{A})$[10], where L is the longest edge of τ and A is its area. If we choose the same parameter α to generate the Poisson disc sampling $\mathcal{P}_\alpha$ and use it to build the solid α-complex $\mathcal{C}_\alpha$, we prove that all triangles $\tau \in \mathcal{C}_\alpha$ have aspect ratio less or equal than $4\sqrt{3}$, which is only three times the aspect ratio of an equilateral triangle. We also found a sampling condition on parameter α of the Poisson disc sampling where its reconstruction by means of the solid α-complex is topologically equivalent to $\mathcal{O}$. As we will see later, such condition is half of the smallest local feature size of $\partial\mathcal{O}$.

Related Works The paper of Amenta and Bern[20] introduced the notion of ϵ-*sampling* which provides mathematical framework for the problem of reconstruction of surfaces. Our goal is to apply Poisson disc sampling (a class of ϵ-sampling) on solid objects instead of surfaces. These details rather change the problem approach.

The work of Edelsbruner et al[7] studies the problem of constructing simplicial complexes that represents or approximate a geometric object of some finite-dimensional Euclidean spaces $\mathbb{R}^d$. As a research direction, they propose the design of methods that choose finitely many points resulting in good quality discretizations of a subspace domain $\mathbb{X} \subset \mathbb{R}^d$. We tackle this problem exactly in the two dimensional Euclidean space.

In Carlssons and Silva[22] is introduced *witness complexes* which allows approximation of the topology of a point cloud at different scales. In some sense, the solid α-complex of Poisson disc samples also provides an approximation of the object at the scale given by the discs size.

In Frosini[17] it is discussed an algorithm for the computation the *size functions*. It applies a technic to ensure that a curve α is covered by open circles in such a way that each circle contains exactly one arc of α. Our paper uses a similar approach in a more general definition of Poisson disc samplings and in the proof of theorem 2, which establishes the sampling condition for topological equivalence.

Paper outline In the next section we construct the theoretical framework by giving some basic concepts such as simplicial complex, Delaunay triangulation, α-complex and solid α-complex. We also give preliminary notations. In Section 3 we define Poisson disc sampling and show how to generate it. In Section 4 we prove the quality theorem giving an analytic and numeric proof. In Section 5 we establish the α-value sampling condition with topological guarantees. In Section 6 we discuss some experimental results and in Section 7 we finalize the paper with a conclusion.

2. Concepts and Preliminary Notations

2.1. *Simplicial Complex*

A *simplex* σ^p of dimension p (p-simplex, for short) is the convex hull of $p+1$ points $\{v_0, ..., v_p\}$, when the points $v_i \in \mathbb{R}^n$ are in general position, i.e., the vectors $v_1 - v_0, v_2 - v_0, ..., v_p - v_0$ are linearly independent. The points $v_0, ..., v_p$ are called the *vertices* of σ. The simplices of dimensions 2 and 1 will be called, respectively, *triangles* and *edges*.

A *face* of σ is the convex hull of some of the vertices of σ. It is then also a simplex.

A *simplicial complex* K is a finite set of simplices together with all its subsimplices such that if σ and τ belong to K, then either σ and τ meet at a subsimplex λ, or $\sigma \cap \tau = \emptyset$. The dimension of a simplicial complex K is the highest dimension of its simplices. If a collection of simplices $L \subset K$ is a simplicial complex, then L is called a *subcomplex* of K. The *underlying polyhedron* $|K| \subset \mathbb{R}^n$ corresponds to the union of the simplices in K.

An m-dimensional *solid simplicial complex* L is a simplicial complex of dimension m that has no isolated simplices, where an *isolated simplex* is a p-simplex, with $p < m$, that is not a face of an m-simplex in L. Given a m-dimensional simplicial complex K, the *maximal solid simplicial complex* of K, denoted by $\overline{K}$, is the subcomplex of K that contains all the m-simplices of K.

The previous definition of the solid complex is a class of the *closed regular set (r-sets)*[23], i.e., a set that equals the closure of its interior. More precisely, given a solid complex $\overline{K}$ then $|\overline{K}|$ is a finite r-set.

2.2. *Delaunay Triangulations*

A *Delaunay triangulation*[18] of a set of points in the plane is a unique set of triangles connecting the points that satisfies the "empty circle" property: the circumcircle of each triangle does not contain any other points of the set. It is in some sense the most natural way to triangulate a set of points since it best approximates the second order geometry of the points.

Definition 1. Given a set $S \subset \mathbb{R}^n$ of points in general position, the Delaunay Triangulation of S is the simplicial complex $\mathrm{DT}(S)$ consisting only of

(1) all k-simplices, $(0 \leq k \leq n)$, with $T \subset S$ such that the circumsphere of T does not contain any other point of S, and
(2) all k-simplices which are faces of other simplices in $\mathrm{DT}(S)$.

2.3. *α-Complex*

An *α-complex*[5,6] is a subcomplex of the Delaunay triangulation that mainly contains only the triangles of circumsphere radius lower than a positive real parameter α. More precisely:

Definition 2. Let $S \subset \mathbb{R}^n$ be a set of points in general position. For $T \subset S$ with $\#T \leq n$, let b_T and μ_T denote the smallest ball that contains the points of T and its radius, respectively. Given a parameter $0 \leq \alpha \leq \infty$, the *α-complex* $\mathcal{C}_\alpha(S)$ of S is the subcomplex of $\mathrm{DT}(S)$ made of simplices σ_T in $\mathcal{C}_\alpha(S)$ such that:

(1) either $\mu_T < \alpha$ and $b_T \cap S = \emptyset$,
(2) or σ_T is a face of another simplex in $\mathcal{C}_\alpha(S)$.

For large values of the parameter α, the α-complex coincides with the Delaunay triangulation.

2.4. *Solid α-Complex*

Since the α-complex $\mathcal{C}_\alpha$ may contain isolated simplices, let us define the *solid α-complex* as the maximal solid simplicial complex of $\mathcal{C}_\alpha$, denoted by $\overline{\mathcal{C}_\alpha(\mathcal{S})}$. This approach was also inspired by Bernardini et al[8], which defined the *α-solid* as the polytope that "regularizes" the α-shape[5]. Since we are dealing with meshes we adapted this definition to simplicial complexes.

In the literature, most of the algorithms computes the Delaunay triangulation as an intermediate stage to get the α-complex. However, we can apply the ball-pivoting algorithm restricted to the plane (RBPA)[12] to build the solid α-complex in linear time on the number of points without having to calculate previously the Delaunay triangulation.

3. Poisson Disc Samplings

In this section we will define Poisson Disc Samplings (PDS), a class of stochastic samplings widely used in discrete geometry applications. These samplings are easily generated for, at least, planar regions R that are open, connected and bounded. In a Poisson disc sampling, the sample points must satisfy two desired characteristics which match with the requirements for good numerical approximations: the sample has a minimum proximity and are well spread over the considered region.

Definition 3. For $\alpha > 0$, let $P_\alpha = \{p_1, p_2, ..., p_n\}$ be a sampling of a solid region $R = A \cup \partial A$, where A is a bounded, open and connected subset of the plane. We say that P_α is a Poisson Disc Sampling if it satisfies:

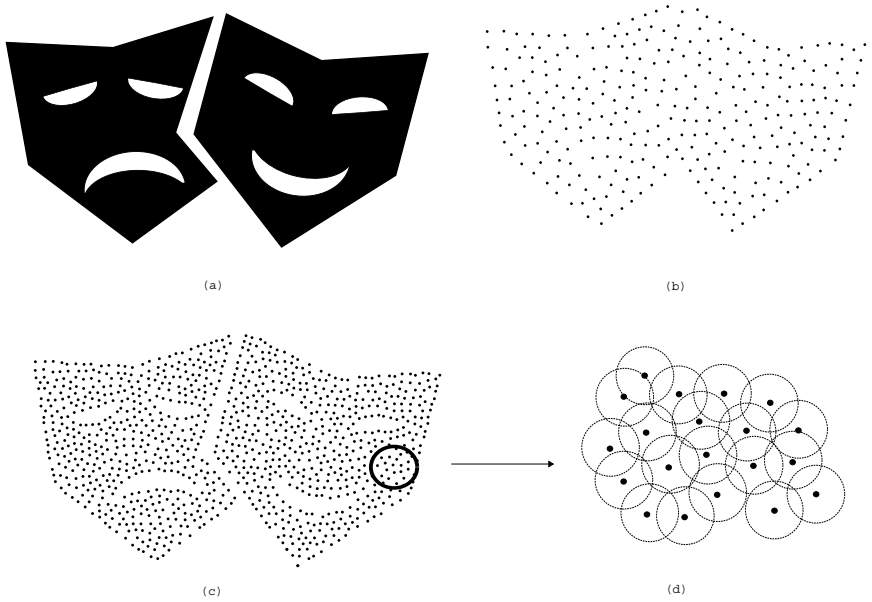

Figure 1. (a) Two connected components regions (tragedy–comedy masks). (b) Coarse sampling. (b) Fine sampling. (d) Zooming samples with Poisson discs.

(1) *[Coverage condition]* the region R is covered by the balls of radius α centered at the sampled: $R \subset \cup_{p_i \in P_\alpha} B_\alpha(p_i)$, and
(2) *[Poisson condition]* any two points are separated by a distance greater than α :$P_\alpha \cap B_\alpha(p_i) = \{p_i\}$, $\forall i$.

Proposition 1. *There exists a PDS for any region R.*

Proof. The sampling can be generated by the algorithmic approach of *dart throwing*[1]. In this approach we have a random sample generator in the region and a validation procedure that checks if the samples satisfy the desired geometric criteria. In our case the criteria is the Poisson condition. If a sampling is validated then we add it to the output, otherwise, we discard it. The algorithm stops when all samplings satisfy the covering condition. In the figure 1 we have an example of PDS. □

4. Aspect Ratio Bound

4.1. *Aspect ratio*

To study the quality of the mesh generated by computing the solid α-complex of a Poisson disc sampling, we adopt a triangle shape metric[9]. A popular one for a triangle τ is its aspect ratio $(\frac{L^2}{\text{Area}(\tau)})$[10], where L is the longest edge of τ.

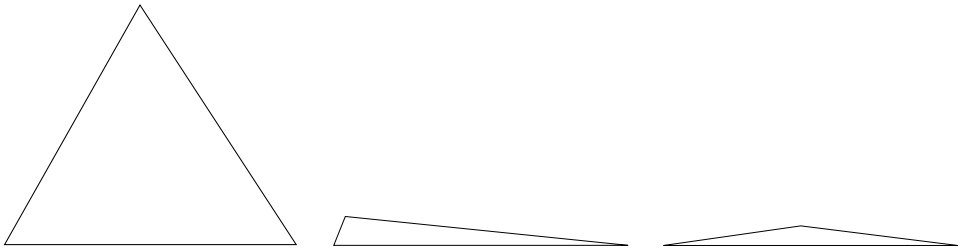

Figure 2. Triangle aspect-ratio: well-shaped (left) and degenerate triangles (right).

The aspect ratio of an equilateral triangle is $\frac{4}{3}\sqrt{3}$ and that it is the minimal one. This corresponds to the intuition that the equilateral triangle is the best shaped one. Then, the lower its aspect ratio, the closer to an equilateral triangle is (cf. Figure 2).

4.2. *Intuitive bound*

Triangles with large aspect ratio are degenerated, and they contribute to numerical instabilities in simulations. In the center of Figure 2, the triangle is degenerated since two of its vertices are too close. This case cannot occur in an solid α-complex of a PDS because of the Poisson condition. Therefore in our context, the only possibility is the one at the right of Figure 2. The thinner is the triangle, the greater is its circumradius. Since the parameter α of the PDS also serves for the solid α-complex, its construction removes such triangles with large circumradius from the Delaunay triangulation. Then, we expect that the solid α-complex of a PDS has an upper bound for the aspect ratio of its triangles. It is also intuitive from previous results that well spaced points imply bounded aspect ratio. [14,15]

4.3. *The Quality Theorem*

In this section, we will show the first result of the paper, i.e., an aspect ratio upper bound in a given solid α-complex of a PDS. This bound is $4\sqrt{3}$, which is only three times the aspect ratio of an equilateral triangle. Moreover, we prove that this bound is tight.

Theorem 1. *Let P_α be a PDS sampling of a region R. The aspect ratio of the triangles of $\overline{C_\alpha(P_\alpha)}$ is bounded by $4\sqrt{3}$.*

Proof. Let τ be a triangle and $b \leq a \leq L$ its three edge lengths. Let $S(\tau)$ be the area of the triangle τ and R its circumradius. Using, $S(\tau) = \frac{abL}{4R}$, we get aspect-ratio$(\tau) = \frac{L^2}{S(\tau)} = \frac{4RL}{ab}$. We will look for the worst case, i.e. the triangle that have the biggest possible aspect ratio, with the restriction $L > a > b \geq \alpha$ (PDS condition) and $R \leq \alpha$ (solid α-complex condition).

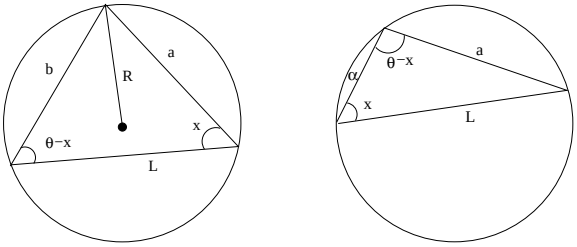

Figure 3. Minimizing ab with R and L fixed (left) and maximizing $\frac{L}{a}$ with R and $b = \alpha$ fixed (right).

Worst case: $b = \alpha$

We first check that the smallest edge b may actually reach the smallest distance between points, i. e., α. Fix R and L, the worst aspect ratio will be obtained minimizing ab. Using the notation of Figure 3 (left), we have:

$$\frac{a}{\sin(\theta - x)} = \frac{b}{\sin x} = \frac{L}{\sin(\pi - \theta)} = k,$$

where k is a constant fixed by R and L. This implies that:

$$ab = k^2 \sin(x) \sin(\theta - x).$$

Differentiating $f(x) = \sin(x)\sin(\theta - x)$ we obtain:

$$f'(x) = \cos(x)\sin(\theta - x) - \cos(\theta - x)\sin(x) = \sin(\theta - 2x).$$

Since b is the smallest edge, $\sin(\theta - x) \geq \sin(x)$, where $\frac{\pi}{2} \geq \theta - x \geq x$, and we have $\sin(\theta - 2x) \geq 0$. We conclude that f is a non decreasing function, and the minimum value of the product ab occurs at the minimal value of b. However, the PDS condition ensures that $\alpha \leq b$. Then, the lowest value of ab takes place at $b = \alpha$.

Worst case: $a = b = \alpha$

Now let us check that a can also reach α, the minimal value for ab being α^2. The worst aspect ratio will occur when the ratio $\frac{L}{a}$ is maximal. Fix R and $b = \alpha$, using the notation of Figure 3 (right) we have:

$$\frac{L}{a} = \frac{\sin(\theta - x)}{\sin x} = \sin\theta \cot x - \cos\theta.$$

Since $0 \leq x \leq \frac{\pi}{2}$ and since the cotangent function is decreasing, the maximal value of the ratio occurs when a is minimal, i.e. $a = \alpha$.

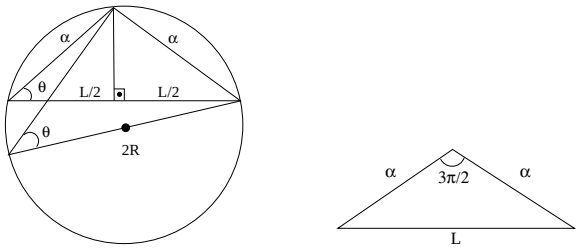

Figure 4. Maximizing RL with $a = b = \alpha$ fixed (left) and the worst case configuration (right).

Worst case: $a = b = R = \alpha$

To get the worst aspect ratio we maximize RL, fixing $a = b = \alpha$. Using the notation of Figure 3(left) we have that:

$$\cos\theta = \frac{L}{2\alpha} \quad , \quad \sin\theta = \frac{\alpha}{2R}. \text{ then } \frac{L^2}{4\alpha^2} + \frac{\alpha^2}{4R^2} = 1.$$

We get:

$$(4\alpha^2 - L^2) \cdot R^2 = \alpha^4.$$

Since RL is maximal when R is maximal, i.e. $R = \alpha$, since $R \leq \alpha$ from the solid α-complex condition. The above relation then defines $L = \alpha\sqrt{3}$. □

The maximal aspect ratio is $4\sqrt{3}$ which is the configuration of the triangle of the Figure 3(left). In this case the greatest angle is $\frac{3\pi}{2}$. This proves that the upper bound is tight.

4.4. *A Numerical Proof*

We can verify the upper bound by optimizing an objective function using the Maple software. The problem can be modeled as:

$$\min_{a,b,L}(-\frac{L^4}{A^2}) \tag{1}$$

s.t.

$$a \leq \alpha,\ b \leq \alpha \text{ and } R^2 \leq \alpha^2.$$

where by the known Heron's formula we have $A^2 = p(p-a)(p-b)(p-L)$, with $p = \frac{a+b+L}{2}$. For parameter radius R we find again $R = \frac{abL}{4A}$. Our problem can be solved using Lagrangian multipliers with KKT conditions. For $x = (a, b, L)$ and $\mu = (\mu_1, \mu_2, \mu_3)$, the Lagrangian of the constrained optmization problem is:

$$f(x,\mu) = -\frac{L^4}{A^2} + \mu_1 \cdot \underbrace{(\alpha - a)}_{h_1} + \mu_2 \cdot \underbrace{(\alpha - b)}_{h_2} + \mu_3 \cdot \underbrace{(\alpha^2 - \frac{a^2 b^2 L^2}{16A^2})}_{h_3} \tag{2}$$

which gives optimality conditions for $x^* = (a^*, b^*, L^*)$ and $\mu^* = (\mu_1^*, \mu_2^*, \mu_3^*)$ as a local minimum:

(1) $\bigtriangledown_x(L(x^*, \mu^*)) = 0$
(2) $\mu^* \geq 0$
(3) $\mu_i^* \cdot h_i(x^*) = 0$, where h_i is defined in equation 2.

Since there are three complementary conditions we have eight cases to check. The only feasible case results in $\{a = \alpha, b = \alpha, c = \alpha\sqrt{3}\}$.

5. Sampling Condition

Consider a region R and its PDS P_α. In this section we will prove that for a sufficiently small parameter radius α the polytope $|C_\alpha(P_\alpha)|$ is topologically equivalent to R.

Definition 4. The *Medial Axis* of the boundary ∂R is the closure of points in the plane which have two or more closest points in ∂R.

The *Local Feature Size* function quantifies the local level of detail at a point on smooth curve.

Definition 5. The *Local Feature Size*, $LFS(p)$, of a point $p \in \partial R$ is the Euclidian distance from p to the closest point m on the medial axis.

Notice that, because it uses the medial axis, this definition of local feature size depends on both the curvature at p and the proximity of nearby features.

Now we will enunciate and prove five lemmas before the theorem 2.

Lemma 1. *A disk containing a point $p \in \partial R$, with diameter at most $LFS(p)$, intersects ∂R in a topological interval.*

Proof. See Amenta et al [19]. □

Lemma 2. *Let R be a region and P_α a PDS such that*

$$\alpha \leq \frac{1}{2} \min_{p \in \partial R} LFS(p) \tag{3}$$

then $C_\alpha(P_\alpha) = \overline{C_\alpha(P_\alpha)}$.

Proof.

According to definition of solid simplicial complexes we have two cases. They correspond to the property that $C_\alpha(P_\alpha)$ does not contain isolated simplices.

First case: $C_\alpha(P_\alpha)$ does not have isolated points.

Suppose that p is an isolated point. Then we have that:

$$B_\alpha(p) \cap (\bigcup_{q \in P_\alpha,\ q \neq p} B_\alpha(q)) = \emptyset$$

Let $w \in P_\alpha - \{p\}$. As R is connected there exists a path pw contained in R. But this is an absurd because there is a ϵ ring neighborhood of $B_\alpha(p)$ that does not contain any point of R and pw must pass through this ring.

Note that we proved this first result by using only connectivity arguments which means that, independently of α $C_\alpha(P_\alpha)$, is always a connected graph.

Second case: $C_\alpha(P_\alpha)$ does not have isolated edges.

Suppose that e is an isolated edge and let p and q be its vertices. Let $\{x, y\} = \partial B_\alpha(p) \cap \partial B_\alpha(q)$. We will show that $\{x, y\}$ are outside. Suppose $x \in R$ then by the coverage condition there exists a point $r \in P_\alpha$ such that $x \in B_\alpha(r)$. Then we have that $B_\alpha(r) \cap B_\alpha(p) \cap B_\alpha(q) \neq \emptyset$ and we conclude that the circumscribed circle of the triangle pqr has radius less or equal than α and it does belong to $C_\alpha(P_\alpha)$. This is an absurd because we have supposed that e is isolated. Hence $x \notin R$. Using the same arguments we can prove that $y \notin R$.

As a consequence of the intermediate value theorem the line segment px intersects ∂R in some point x'. Analogously for the line segments qx, py and qy we have the boundary points x'', y' and y''.

Take a circle with diameter $x'x''$. It is easy to see that size $|x'x''| < 2\alpha$. Using the fact that $2\alpha < LFS(z)$ for all z in ∂R and applying the lemma 1 we have that this circle intersects ∂R in a topological interval. Lets denote this interval as $[x', x'']$. Analogously we get the intervals $[x'', y'']$, $[y'', x']$ and $[y', x']$. All these interval joined compose the closed boundary Γ. Since the interval $[x'', y'']$ is also part of the interval of the disc $B_\alpha(q)$ it separates this disc into two regions, one in the interior of R and other in the exterior of R. As p is an interior point then the interval $[x'', y'']$ must intersect the circle C with diameter pq at least in two distinct points a and b in order to contain the point q. Analogously $[x', y']$ intersects C in more two points b and c. We have that $pq < 2\alpha$ and, again, using the lemma 1, C intersects ∂R in an interval. This is an absurd because every interval has only two extremes and we found at least four, that is, a, b, c and d.

This lemma show us that $C_\alpha(P_\alpha)$ is a solid object. □

Lemma 3. *Let R be a region and P_α a PDS such that inequality (3) is satisfied. If p and q are two boundary points such that $B_\alpha(p) \cap B_\alpha(q) \neq \emptyset$ then $(B_\alpha(p) \cup B_\alpha(q)) \cap \partial R$ is a topological interval.*

Proof.

Suppose that $B_\alpha(p) \cap B_\alpha(q) \cap \partial R$ is not a topological interval. We will take an argument similar to the one used in the preceding lemma. The interval $I = B_\alpha(p) \cap \partial R$ splits the disk $B_\alpha(p)$ into two regions, one interior of R and other exterior. As p is inside R then the boundary of the circle C with diameter pq intersects I in two points a and b. In the same way the interval $I' = B_\alpha(q) \cap \partial R$ intersects the boundary of C in two points c and d. The circle C has diameter less than α and it intersects ∂R in a topological interval. This is an absurd because ∂C has four intersection points with ∂R, that is a, b, c and d.

In conclusion, given B_i a boundary component of R then it is covered by a closed chain of circles, that is, its dual graph is homeomorphic to B_i. □

The next definition will assign topology information to sampling points. It will be used to prove the following lemma.

Definition 6. Let P_α be a PDS of a region R and $p \in P_\alpha$ a sample point. We say that p is *boundary* if $B_\alpha(p) \bigcap \partial R \neq \emptyset$, otherwise, we say that p is *interior*.

Lemma 4. *Let R be a region and P_α a PDS such that inequality (3) is satisfied. Given $p \in P_\alpha$, if p is interior then p is in the interior of $C_\alpha(P_\alpha)$.*

Proof. Since p is an interior point then the disk $B_\alpha(p)$ is all contained in R. Let $A \subset P_\alpha$ be a set of points such that

$$\partial B_\alpha(p) \subset \bigcup_{q \in A} B_\alpha(q)$$

The points in A falls exactly in the link of p and they are connected. Then p lies in the interior of $C_\alpha(P_\alpha)$. □

Lemma 5. *Let R be a region and P_α a PDS such that inequality (3) is satisfied. The region R and $|C_\alpha(P_\alpha)|$ have the same number of boundary components.*

Proof. We will establish a bijection between the boundary components of R and $|C_\alpha(P_\alpha)|$.

Consider B_i a boundary component of ∂R. By lemma 3 there exists a chain of circles covering this component such that its dual graph C_i is homeomorphic to B_i.

Let C_i be a boundary component of $|C_\alpha(P_\alpha)|$. By lemma 4 a interior point $p \in P_\alpha$ is in the interior of $|C_\alpha(P_\alpha)|$ then we conclude that C_i has only boundary points of the same connected component. Hence C_i is assigned directly with the boundary such that its points belong. □

Theorem 2. *Let R be a region and P_α a PDS such that inequality (3) is satisfied. Then $|C_\alpha(P_\alpha)| \sim R$. The symbol $\sim$ means that the two spaces are topologically equivalent.*

Proof. Since R and $|C_\alpha(P_\alpha)|$ are solid objects then they have the same number of connected components. It is well known that this result implies they are topologically equivalent. □

Additionally to the theorem above we have the equality $C_\alpha(P_\alpha) = \overline{C_\alpha(P_\alpha)}$. Moreover, the complex $C_\alpha(P_\alpha)$ is *combinatorial manifold*, i.e., every boundary vertex bounds only two edges.

6. Examples

In Figure 5, we compare the quality of two triangulations generated from two different PDS samplings of the same rectangular region. We check that the quality of the triangles does not depend on a specific PDS and that the aspect ratio is more concentrated on the left of the histogram which is fair. We also have the numerical statistics of the average, standard deviation, minimum and maximum. The low standard deviation indicates that the data is little spread around the average as well the minimum and maximum validate the aspect ratio interval bounds argued in this article.

In figure 6, we have two regions sampled in two different resolutions. The first region 6(a) has the topology defined by two holes. They are two circles such that the biggest circle's radius is approximately the quadruple of the lesser circle's radius. Having the first sampling parameter α as half of the biggest circle's radius, we observe in 6(b) that the α-complex, as expected by theorem 2, captures only the topology of this circle. As we decrease the parameter α to half of the lesser circles radius then, as we can see in figure 6(c), the α-complex captures the whole topology. In the second region 6(d) there is one hole such that its shape is composed by two identical circles joined by a rectangular pipe. In figure 6(e), when we choose the parameter α as half of the minor circle's radius the α-complex captures only the topology of the circles. As we decrease the parameter by half of the height of the pipe, then in figure 6(f) we check that the whole topology is recovered.

7. Conclusion

In this paper, we proved two results on solid α-complex on Poisson disc samplings. In the first one we showed that the triangles of a 2D solid α-complex have limited aspect ratio. More precisely we proved that the upper bound is $4\sqrt{3}$ and the equality occurs for isosceles triangles when the greater angle is $\frac{3\pi}{2}$. In the second result we showed a sampling condition on parameter α of the Poisson disc sampling to reconstruct the solid object R with topological guarantees. If α satisfies the inequality 3 then the polytope $|C_\alpha(P_\alpha)|$ is topological equivalent to R.

The aspect ratio bound is not directly extendible for dimension three. A simple counter-example involves a sliver tetrahedron, generated by perturbing four samples on the vertices of a square. This tetrahedron locally satisfies the PDS condition but it has an aspect ratio arbitrarily large.

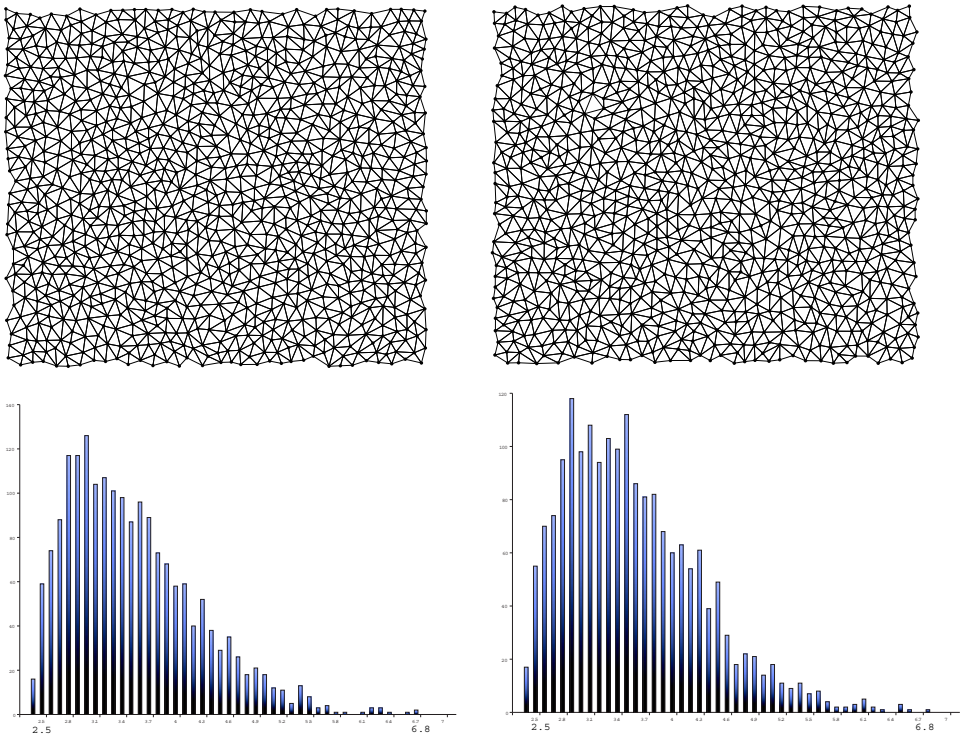

Example	Average	Standard Deviation	Minimum	Maximum
Left	3.46	0.73	2.31	6.68
Right	3.52	0.75	2.32	6.70

Figure 5. Two Poisson disc samples with the same parameter α and the corresponding aspect ratios distributions.

We conjecture that the theorem 2 may be generalized for n-dimensional Euclidean space. The **min** constraint for local feature size of the boundary is very strong because it turns the sampling condition a global parameter. A natural way to reconstruct the whole object adaptively is to unify a formalization of adaptive Poisson disc samplings[24] with the witness complexes[22]. Possibly, it give good results both in geometric quality and in topology recovery.

The examples of Figure 6 may be applied in multiresolution modeling of solid objects. As we increase the sampling rate, we are able to identify two types of details that are emphasized: the geometrical features characterized by the shape of the holes and the features characterized by the number of holes. The last one is what we call "topological" features. For more details on this work, see Medeiros[12].

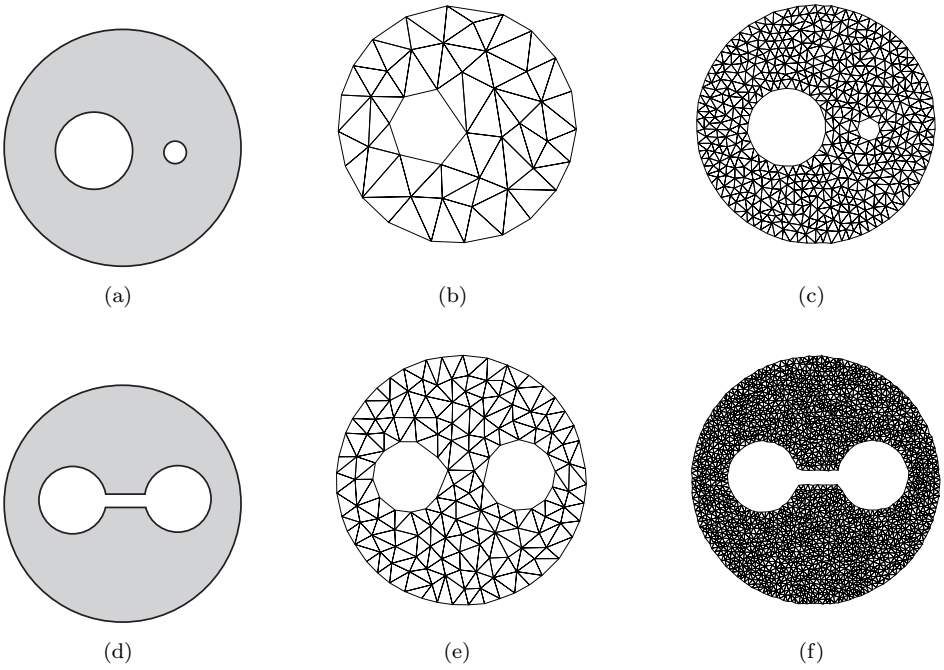

Figure 6. Examples of Poisson disc samples in multiresolution on two different regions and their solid α-complexes.

Acknowledgements

The VISGRAF Laboratory at IMPA is sponsored by CNPq, FAPERJ, FINEP and IBM Brasil. The Matmidia Laboratory at PUC-Rio is sponsored by CNPq and FAPERJ.

Bibliography

1. R. L. Cook. *Stochastic Sampling in Computer Graphics*. ACM Transactions on Graphics, 5(1):51-72, 1986.
2. S. Hiller and O. Deussen. *Tiled Blue Noise Samples*. In: Vision, Modeling, and Visualization, IOS Press, pp. 265–271, 2001.
3. J. I. Yellot 1983. *Spectral Consequences of Photoreceptor Sampling in the Rhesus Retina*. Science 221 , 382–385.
4. J.-D. Boissonnat, L. J. Guibas, and S. Y. Oudot. *Manifold Reconstruction in Arbitrary Dimensions using Witness Complexes*, Proc. 23rd ACM Sympos. on Comput. Geom., pages 194–203, 2007.
5. H. Edelsbrunner and E. P. Mucke, *Three-dimensional α-shapes*, ACM Transactions on Graphics, 10(1):43–72, 1994.
6. H. Edelsbrunner, D. G. Kirkpatrick, and R. Seidel, *On the shape of a set of points in the plane*. IEEE Transactions on Information Theory, 29:521–559, 1983.

7. H. Edelsbrunner and N. R. Shah, *Triangulating Topological Spaces. International Journal of Computational Geometry & Applications*, 7:365–378, 1997.
8. F. Bernardini, C. Bajaj, J. Chen and D. Schikore. *Automatic Reconstruction of 3D CAD Models form Digital Scans*. Computational Geometry and Applications, 9(4–5):327–370, 1999.
9. P. J. Frey and H. Borouchaki. *Surface Mesh Quality Evaluation.* Numerical Methods in Engineering, 45:101–118, 1999.
10. S. W. Cheng. *On the Sizes of Delaunay Meshes.* Computational Geometry, 33:130–138, 2006.
11. D. Eppstein. *Global optimization of mesh quality.* Meshing Roundtable Tutorial, 2001.
12. E. Medeiros, L. Velho and H. Lopes. *Restricted BPA: Applying Ball-Pivoting on the Plane*. In: Sibgrapi, 2004.
13. E. Medeiros. *Solidy Topology in Multiresolution*. PhD Thesis, Instituto de Matemática Pura e Aplicada, Rio de Janeiro, 2009.
14. J. Ruppert. *A New and Simple Algorithm for Quality 2-Dimensional Mesh Generation.* In: ACM-SIAM Symposium on Discrete Algorithms, pp. 83–92, 1993.
15. C. Zhu, G. Sundaram, J. Snoeyink, J. S. B. Mitchell. *Generating Random Polygons with Given Vertices.* Computational Geometry, 6(5):277–290, 1996.
16. D. Dunbar, G. Humphreys. *A Spatial Data Structure for Fast Poisson-Disc Sample Generation.* In: Siggraph, 2006.
17. Frosini, P. *Discrete Computation of Size Functions.* Journal of Combinatorics, Information & System Sciences, 17, 3–4 , pp. 232–250, (1992).
18. F. P. Preparata and M. I. *Shamos Computational Geometry: an Introduction*, Springer-Verlag, 1985.
19. N. Amenta, M. Bern D. Eppstein. *The Crust and the β-Skeleton: Combinatorial Curve Reconstruction*. Graphical Models and Image Processing, 60/2:2, pp. 125–135, 1998.
20. N. Amenta and M. Bern. Surface reconstruction by Voronoi filtering. Discrete Comput. Geom., 22(4):481504, 1999.
21. P. G. Ciarlet, *Basic Error Estimates for Elliptic Problems*, Handbook of Numerical Analysis, vol II, Finite Element Methods (Part I), pp. 17–352, North Holland, 1991.
22. V. de Silva, G. Carlsson, *Topological estimation using witness complexes*, Symposium on Point-Based Graphics, ETH, Zrich, Switzerland, June 24, 2004.
23. A. Requicha *Mathematical Models of Rigid Solid Objects*, Tech. Memo. 28, Production Automation Project, Univ. Rochester, Rochster, N.Y., Nov. 1977
24. L. Feng, I. Hotz, B. Hamann, K. I. Joy. *Anisotropic Noise Samples*. IEEE Trans. Vis. Comp. Graph., 14(2): 342–354, 2008.